The two–photon production quark-antiquark pairs at LHC.

A. Manko, R. Shulyakovsky

Institute of Physics, National Academy of Sciences of Belarus
68 Nezavisimosti av., Minsk, 220072, Belarus,
Institute of Apply Physics, National Academy of Sciences of Belarus
16 Academicheskay st., Minsk, 220072, Belarus

Minsk 2020

Introduction

Major task

Our major task is to calculate total and differential cross sections at the leading order and the next–to–leadint order for the two–photon production quark-antiquark pairs at LHC. These processes are researched at the leading and the next—to—leading order at the elastic case. The total and differential cross sections are obtained. These processes can be used to researched the hadronization quakrs to hadrons and find the effect “new physics”. These process can be to researched for two–photon production hadrons using the quark–hadron duality.

Feynman diagrams and the amplitude of the process $\gamma\gamma \to q\bar{q}$

The following diagram of the processes: $pp \to pW^-W^+p$ and $e^-e^+ \to e^- + W^-W^+ + e^+$ is shown in elastic case: where $P1$ and $P2$ – 4–momentum of initial hadrons or leptons, $P1'$ and $P2'$ – 4–momentum of final hadrons, $k1$ and $k2$ – 4–momentum of q and $\bar{q}$ corresponding.

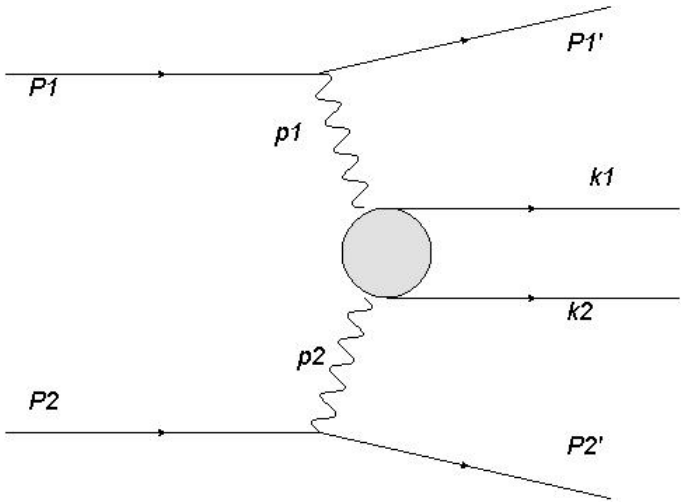

Figure 1: The diagram of the two–photon production the electron–positron pair at LHC

Feynman diagrams and the amplitude of the process $\gamma\gamma \to q\bar{q}$

Leading Order

For example the following diagram of the subprocesses $\gamma\gamma \to u\bar{u}$ is shown in the leading order:

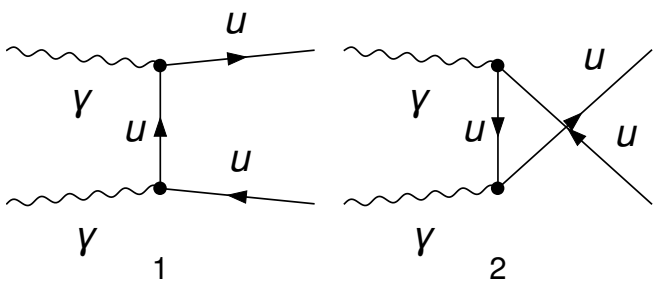

Figure 2: The diagrams of the subprocess in the leading order

Feynman diagrams and the amplitude of the process $\gamma\gamma \to q\bar{q}$

Next–Leading Order

There ate 12 self-energies diagrams. For example the one of these diagrams is shown at this figure.

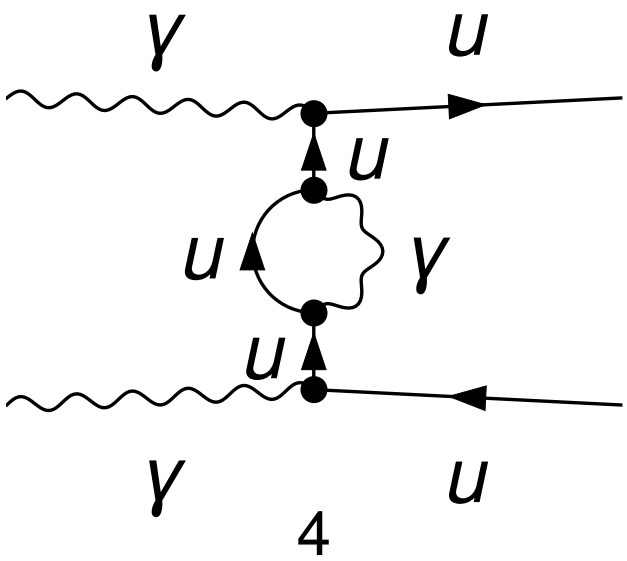

Figure 3: The self–energy diagrams of the subprocess in the next–leading order

Next–Leading Order

There ate 38 boxes diagrams. For example the one of these diagrams is shown at this figure.

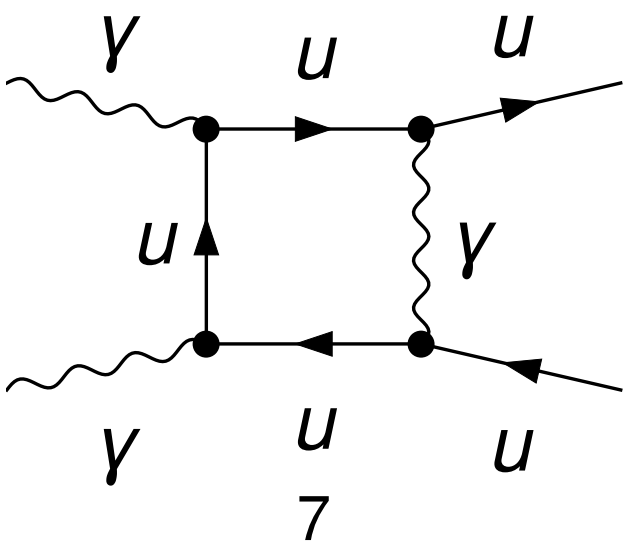

Figure 4: The boxes diagram of the subprocess in the next–to–leading order

Next–Leading Order

There ate 206 boxes diagrams. For example the one of these diagrams is shown at this figure.

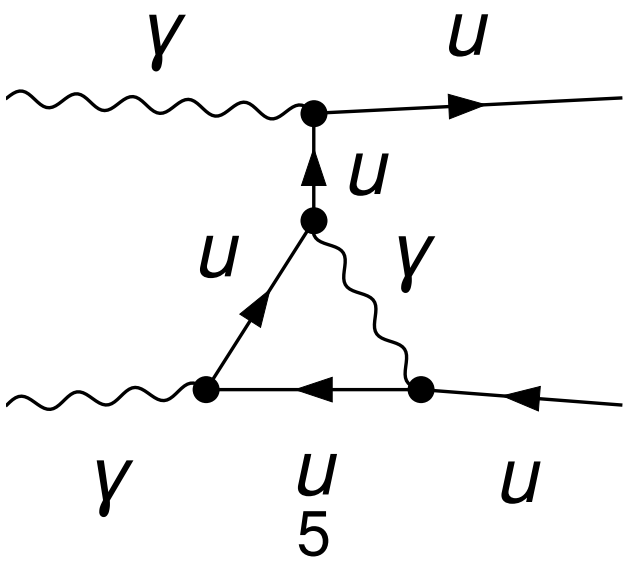

Figure 5: The vertex diagram of the subprocess in the next–to–leading order

Parametrization

The approximation of Weizsacker-Williams(parametrization Budnev and Ginsburg[V.M. Budnev et al., Phys.Rep. 15C (1975) 181]) is used to obtain of total and differential cross sections for the two–photon production lepton pairs. The distribution of photon for protons is given:

$$f_p(x) = \frac{\alpha}{\pi x}\left(1-\frac{1}{x}\right)\left(\varphi\left(\frac{q^2_{max}}{q^2_0}\right)-\varphi\left(\frac{q^2_{min}}{q^2_0}\right)\right), \tag{1}$$

where function φ is

$$\varphi(\xi) = (1+ay)\left(\sum_{k=1}^{3}\frac{1}{k(1+\xi)^k}-\ln(1+\xi^{-1})\right)-\frac{(1-b)y}{4\xi(1+\xi)^3}+c$$
$$\left(1+\frac{y}{4}\right)\left(\ln\left[\frac{1+\xi-b}{1+\xi}\right]+\sum_{k=1}^{3}\frac{b^k}{k(1+\xi)^k}\right), \tag{2}$$

where: $a = 7.16$, $b = -3.96$, $c = 0.028$, $q^2_0 = 0.71\,GeV^2$, $q^2_{max} = 2$, $q^2_{min} = \frac{m_p^2 x^2}{1-x}$, $y = \frac{x^2}{(1-x)}$.

Parametrization

We used Mandelstam variables for a description of the square modulus of the matrix elements of the investigated process, total and differential cross sections. The amplitudes and diagrams of the matrix element were obtained in the program Mathematica using the package FeynArts 3.9. The square module matrix element was obtained in the program Mathematica using the package FeynCalc 9.1.0.

Regularization and renormalization for process $\gamma\gamma \to q\bar{q}$

The dimensional regularization developed by 't Hooft[G. 't Hooft, 1971, Nucl. Phys. B33, 173] and Veltman[G. 't Hooft, M Velman 1972, Nucl. Phys. B44, 189] and the scheme of renormalization developed by A. Denner[A. Denner, Fortsch. Phys. 1993 41, №4 307] were used to calculate the UV- and IR-finite amplitudes. The packages LoopTools was used to calculate numerical loops integrals.

Cuts for the process $\gamma\gamma \to q\bar{q}$

The cuts for ATLAS shown at table 1 were used to calculate total and differential cross section.

Cut	Value
$m_{q\bar{q}}$	24 GeV
p_t	12 GeV
$\lvert\eta\rvert$	2.4
Forward detector: $\lvert\eta_p\rvert$	$4.3 < \lvert\eta_p\rvert < 4.9$

Table 1: The cuts for ATLAS

LHC: total cross section

The total cross section in the elastic case for hadrons colliders is given:

$$\sigma(s) = \int dx_1 \int dx_2 f_p(x_1) f_p(x_2) \hat{\sigma}(x_1 x_2 s). \tag{3}$$

LHC: total cross section: $\gamma\gamma \to q\bar{q}$

There are results of total cross section of the process $\gamma\gamma \to u\bar{u}$ for the leading and the next–to–leading order at LHC at the elastic case at the table 2.

Collider	LO σ pb	NLO σ pb
LHC $\sqrt{s} = 7$ TeV	2.633	2.692
LHC $\sqrt{s} = 8$ TeV	2.757	2.821
LHC $\sqrt{s} = 13$ TeV	3.216	3.293
LHC $\sqrt{s} = 14$ TeV	3.279	3.359

Table 2: Total Cross sections

LHC: total cross section: $\gamma\gamma \to q\bar{q}$

There are results of total cross section of the process $\gamma\gamma \to d\bar{d}$ for the leading and the next–to–leading order at LHC at the elastic case at the table 3.

Collider	LO σ pb	NLO σ pb
LHC $\sqrt{s} = 7$ TeV	1.646	1.804
LHC $\sqrt{s} = 8$ TeV	1.724	1.889
LHC $\sqrt{s} = 13$ TeV	2.008	2.209
LHC $\sqrt{s} = 14$ TeV	2.049	2.247

Table 3: Total Cross sections

LHC: total cross section: $\gamma\gamma \to q\bar{q}$

There are results of total cross section of the process $\gamma\gamma \to s\bar{s}$ for the leading and the next–to–leading order at LHC at the elastic case at the table 4.

Collider	LO σ pb	NLO σ pb
LHC $\sqrt{s} = 7$ TeV	0.1646	0.1723
LHC $\sqrt{s} = 8$ TeV	0.1724	0.1802
LHC $\sqrt{s} = 13$ TeV	0.2008	0.2102
LHC $\sqrt{s} = 14$ TeV	0.2049	0.2144

Table 4: Total Cross sections

LHC: total cross section: $\gamma\gamma \to q\bar{q}$

There are results of total cross section of the process $\gamma\gamma \to c\bar{c}$ for the leading and the next–to–leading order at LHC at the elastic case at the table 5.

Collider	LO σ pb	NLO σ pb
LHC $\sqrt{s} = 7$ TeV	0.2613	0.2990
LHC $\sqrt{s} = 8$ TeV	0.2737	0.3084
LHC $\sqrt{s} = 13$ TeV	0.3189	0.3602
LHC $\sqrt{s} = 14$ TeV	0.3255	0.3753

Table 5: Total Cross sections

LHC: total cross section: $\gamma\gamma \to q\bar{q}$

There are results of total cross section of the process $\gamma\gamma \to b\bar{b}$ for the leading and the next–to–leading order at LHC at the elastic case at the table 6.

Collider	LO σ pb	NLO σ pb
LHC $\sqrt{s} = 7$ TeV	0.1522	0.0.1535
LHC $\sqrt{s} = 8$ TeV	0.1596	0.1608
LHC $\sqrt{s} = 13$ TeV	0.1861	0.1878
LHC $\sqrt{s} = 14$ TeV	0.1900	0.1918

Table 6: Total Cross sections

LHC: differential cross section: $\gamma\gamma \to u\bar{u}$

The differential cross section as a function of the invariant mass of the $u\bar{u}$ for elastic case are shown at figs 8, where the red line – the leading order and the blue line – the next–to–leading order.

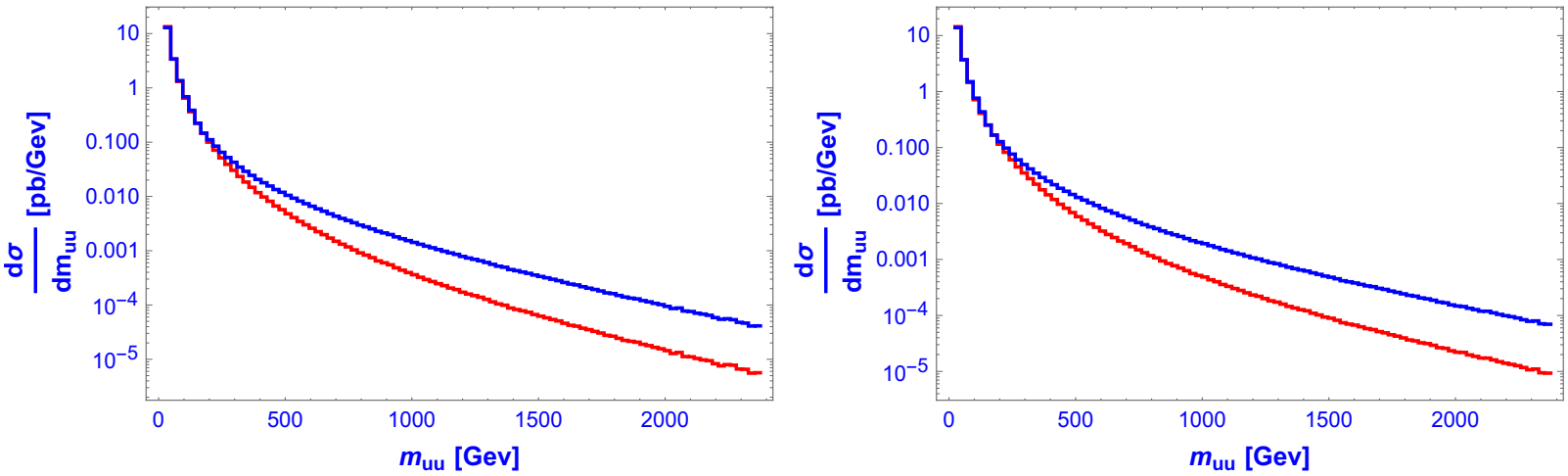

Figure 6: Differential cross section of $u\bar{u}$ production in dependence of the invariant mass of $u\bar{u}$ pair at $\sqrt{s} = 7.0$ TeV (Left) and at $\sqrt{s} = 8.0$ TeV (Right) for elastic case.

LHC: differential cross section: $\gamma\gamma \to u\bar{u}$

The differential cross section as a function of the invariant mass of the $u\bar{u}$ for elastic case are shown at figs 9, where the red line – the leading order and the blue line – the next–to–leading order.

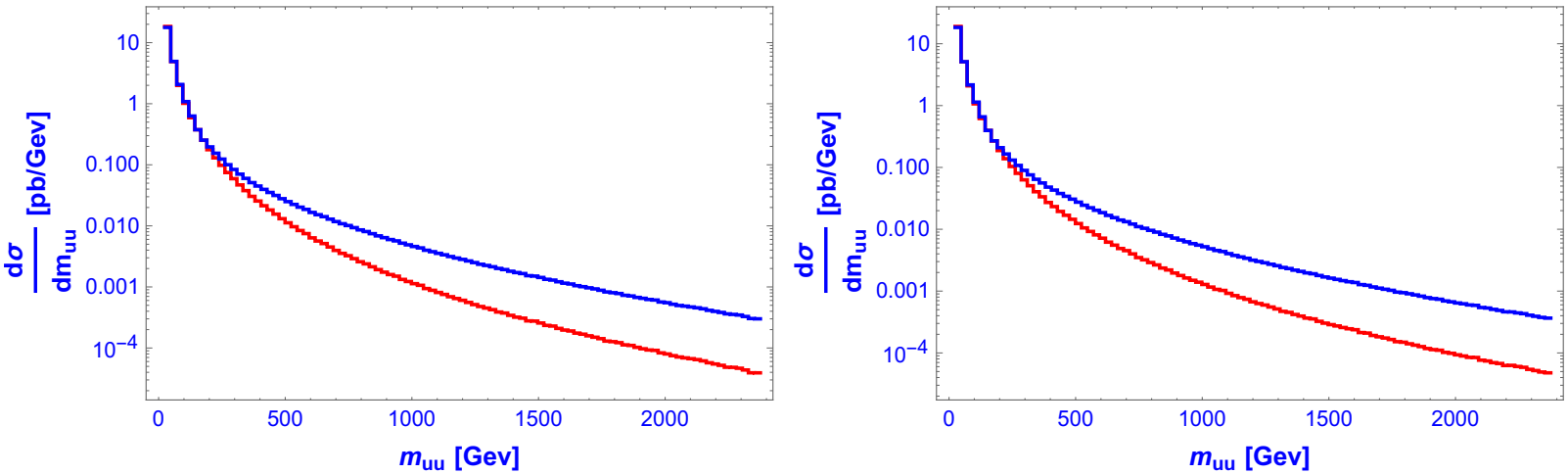

Figure 7: Differential cross section of $u\bar{u}$ production in dependence of the invariant mass of $u\bar{u}$ pair at $\sqrt{s} = 13.0$ TeV (Left) and at $\sqrt{s} = 14.0$ TeV (Right) for elastic case.

LHC: differential cross section: $\gamma\gamma \to d\bar{d}$

The differential cross section as a function of the invariant mass of the $d\bar{d}$ for elastic case are shown at figs 8, where the red line – the leading order and the blue line – the next–to–leading order.

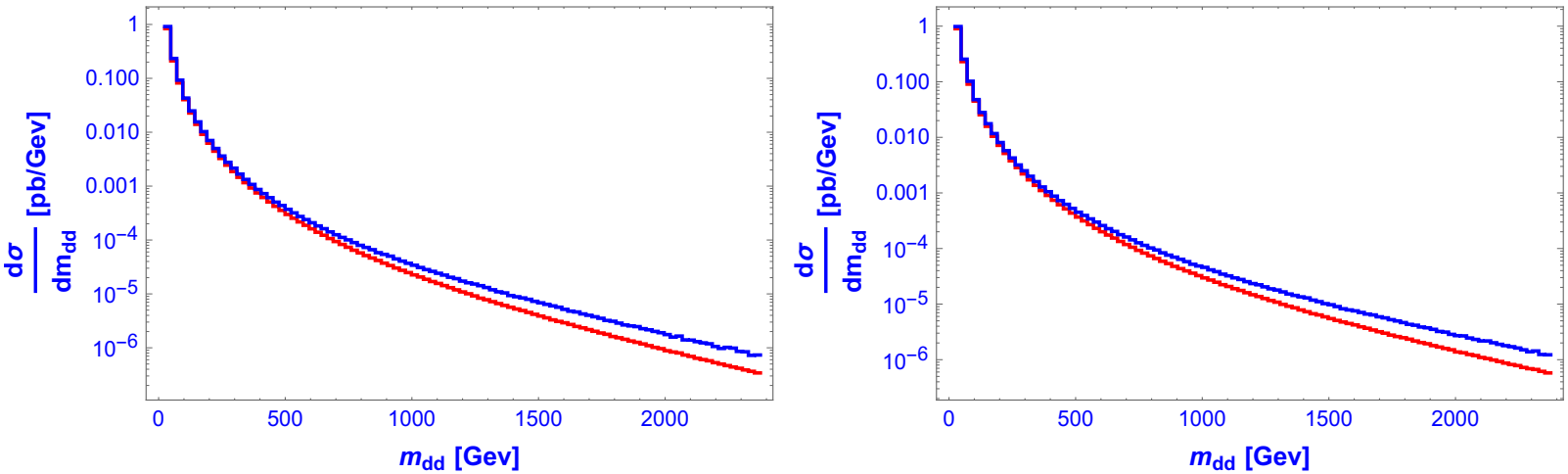

Figure 8: Differential cross section of $d\bar{d}$ production in dependence of the invariant mass of $d\bar{d}$ pair at $\sqrt{s} = 7.0$ TeV (Left) and at $\sqrt{s} = 8.0$ TeV (Right) for elastic case.

LHC: differential cross section: $\gamma\gamma \to d\bar{d}$

The differential cross section as a function of the invariant mass of the $d\bar{d}$ for elastic case are shown at figs 9, where the red line – the leading order and the blue line – the next–to–leading order.

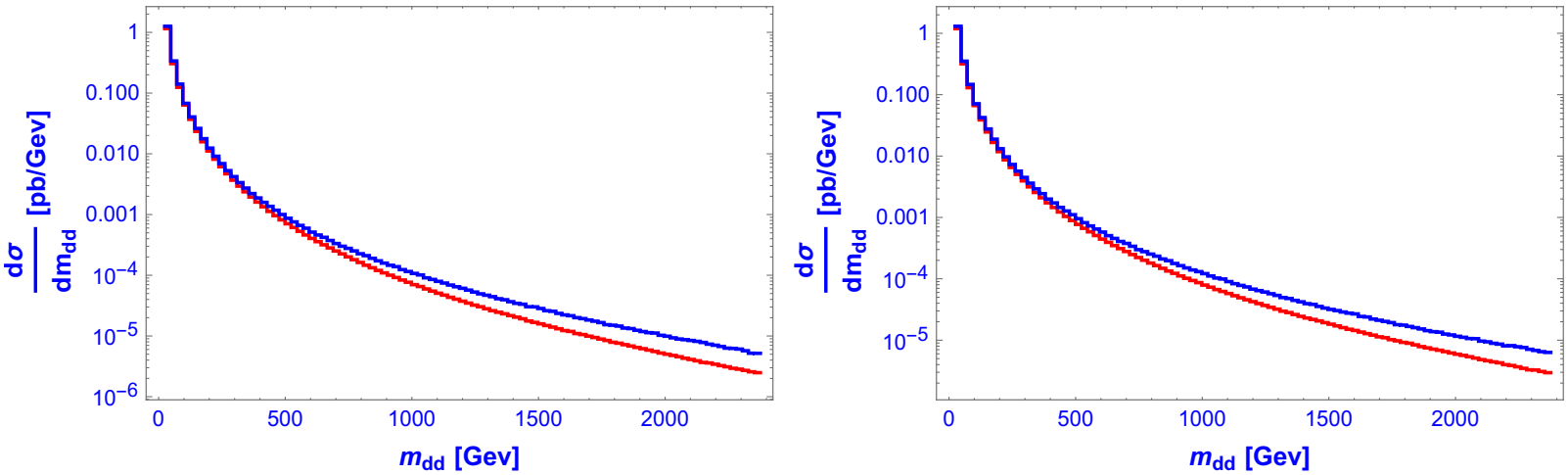

Figure 9: Differential cross section of $d\bar{d}$ production in dependence of the invariant mass of $d\bar{d}$ pair at $\sqrt{s} = 13.0$ TeV (Left) and at $\sqrt{s} = 14.0$ TeV (Right) for elastic case.

Conclusion

We obtained total and differential cross section in the leading and the next–to–leading order for the process of two–photon production quark-anitquark pairs at LHC by using the cuts for the final hadrons(quarks). Total and differential cross sections for two-photon production of quark-anitquark pairs were studied for elastic case at LHC.

Thank you for your attention!